Journal of Hazardous Materials 192 (2011) 722–729

Contents lists available at ScienceDirect

Journal of Hazardous Materials

journal homepage: www.elsevier.com/locate/jhazmat

A kinetic spectrophotometric method for simultaneous determination of phenol and its three derivatives with the aid of artificial neural network

Yongnian Ni[a,b,*], Zhenzhen Xia[b], Serge Kokot[c]

[a] State Key Laboratory of Food Science and Technology, Nanchang University, Nanchang 330047, China
[b] Department of Chemistry, Nanchang University, Nanchang 330031, China
[c] Chemistry, Faculty of Science and Technology, Queensland University of Technology, Brisbane 4001, Australia

ARTICLE INFO

Article history:
Received 26 January 2011
Received in revised form 25 May 2011
Accepted 25 May 2011
Available online 12 June 2011

Keywords:
Kinetic spectrophotometry
Rhodamine B
Phenols
Chemometrics
Water samples

ABSTRACT

A novel kinetic spectrophotometric method was developed for determination of pyrocatechol, resorcin, hydroquinone and phenol based on their inhibitory effect on the oxidation of Rhodamine B (RhB) in acid medium at pH = 3.0. A linear relationship was observed between the inhibitory effect and the concentrations of the compounds. The absorbance associated with the kinetic reactions was monitored at the maximum wavelength of 557 nm. The effects of different parameters such as pH, concentration of RhB and $KBrO_3$, and temperature of the reaction were investigated and optimum conditions were established. The linear ranges were 0.22–3.30, 0.108–0.828, 0.36–3.96 and 1.52–19.76 μg mL^{-1} for pyrocatechol, resorcin, hydroquinone and phenol, respectively, and their corresponding detection limits were 0.15, 0.044, 0.16 and 0.60 μg mL^{-1}. The measured data were processed by several chemometrics methods, such as principal component regression (PCR), partial least squares (PLS) and artificial neural network (ANN), and a set of synthetic mixtures of these compounds was used to verify the established models. It was found that the prediction ability of PLS, PCR and RBF-ANN was similar, however, the RBF-ANN model did perform somewhat better than the other methods. The proposed method was also applied satisfactorily for the simultaneous determination of pyrocatechol, resorcin, hydroquinone and phenol in real water samples.

1. Introduction

The determination of phenol and its derivative compounds is of environmental significance, since these species are important organic contaminants, which occur frequently in ground and surface waters. Due to their toxicity and persistence in the environment, phenols are considered to be priority pollutants. In drinking water, even at low concentration, they give off strong, unusual taste and odor. Also, some of them are thought to be mutagenic [1,2]. Numerous phenolic compounds show toxic effects in animals and plants since they easily penetrate into skin and cellular membrane. Because different phenolic compounds behave differently and have different ecological effects and toxicity, the determination of individual phenolic compounds is particularly important and useful.

There are four common phenolic compounds – hydroquinone, pyrocatechol, resorcin and phenol. The major uses of phenol involve its conversion to plastics or related materials. For example it is commonly used to make bisphenol-A, polycarbonates, and phenolic resins. Phenol is also used in the preparation of cosmetics including sunscreens, hair dyes, and skin lightening preparations [3]. Similarly, resorcin, hydroquinone and pyrocatechol are important industrial substances, and are widely used in polymers, cosmetics, tanning, pesticides, flavoring agents, medicines, and photographic chemicals. Even more significantly, they are generally present in the waste water from oil, paint, polymer and pharmaceutical industries. In addition, they are found in the marine food chain and ultimately, in fish. Thus, the development of reliable and readily accessible procedures for the determination of pyrocatechol, resorcin, hydroquinone and phenol in natural and waste water is currently a topical problem in environmental analysis [4–8].

Several different analytical methods have been proposed for the determination of phenol and its derivatives. The methods widely used are gas chromatography–mass spectrometry (GC–MS) [9], high performance liquid chromatography (HPLC) [10,11], capillary electrophoresis [12], electrochemical methods [4,13], and spectrophotometry [14,15]. However, these methods are sometimes complicated and difficult to reproduce. They are also rather hazardous because they involve some toxic materials and reagents, which can be quite costly.

* Corresponding author at: Department of Chemistry, Nanchang University, Nanchang 330031, China. Tel.: +86 791 3969500; fax: +86 791 3969500.
E-mail addresses: ynni@ncu.edu.cn (Y. Ni), s.kokot@qut.edu.au (S. Kokot).

0304-3894/$ – see front matter © 2011 Elsevier B.V. All rights reserved.
doi:10.1016/j.jhazmat.2011.05.081

Table 1
Chemical structures of phenol and its derivatives.

Material	Molecular formula	Molecular weight	Chemical structures
Pyrocatechol	$C_6H_6O_2$	110.11	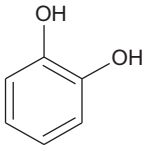
Resorcin	$C_6H_6O_2$	110.11	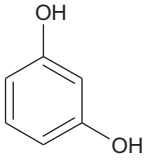
Hydroquinone	$C_6H_6O_2$	110.11	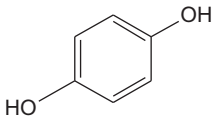
Phenol	C_6H_6O	94.11	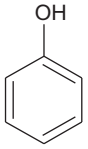

Kinetic methods, including the single point method, the proportional equation model, multivariate calibration, and artificial neural network, is a simple and sensitive analytical technique that can be used for the simultaneous determination of different compounds in various fields [16]. Recently, Fan et al. [5] reported a spectrofluorimetric kinetic method for the determination of trace resorcin, based on the inhibitory effect of resorcin in the oxidation of Rhodamine B (RhB) by potassium bromate in dilute sulfuric acid.

In this study, a rapid, simple and sensitive kinetic spectrophotometric method for the simultaneous determination of traces of phenol and its derivatives (Table 1) in waste water samples was researched and developed. It was based on the inhibitory effect of these trace compounds on the redox reaction between RhB and potassium bromate. This novel method was then applied for the determination of trace phenols in different water samples, and these results were compared with those obtained by the reference HPLC method [17].

2. Theory method

2.1. Different kinetic methods for multicomponent analysis

Consider that a reagent A (here the deep red RhB) reacts with a common reagent R (potassium bromate), under certain conditions to give a decrease in absorbance, A. The reaction of A with R in the absence of any additional analytes such as phenols, can be written as:

$$A + R \xrightarrow{k_1} P_A + Q_R \quad (1)$$

where P_A and Q_R are the corresponding reaction products of A and R, respectively. If $c_R \gg c_A$, the c_R is basically unchanged before and after the reaction, and the reaction rate is only a function of c_A. Thus, the above reaction can be assumed to have pseudo first-order kinetics with respect to concentration A, and the rate equation is:

$$-\frac{d[A]}{dt} = k_1[A] \quad (2)$$

Integration of Eq. (2) yields:

$$\Delta[A]_t = [A]_0 - [A]_t = [A]_0(1 - \exp(-k_1 t)) \quad (3)$$

where $[A]_0$ is the initial concentration of A, $[A]_t$ is the concentration of the product of A at a time, t, $\Delta[A]_t$ is the change in A, and k_1 is the rate constant for reaction (1).

If there are some other compounds present in the solution (except reaction (1)) such as the phenols (D_i, $i = 1, 2, \ldots, I$), the following reaction will also apply:

$$D_i + R \xrightarrow{k_i} P_{D_i} + Q_R \quad (i = 1, 2, \ldots, I) \quad (4)$$

where the P_{D_i} is the oxidized product of compound D_i and k_i is its rate constant for reaction (4).

If $c_R \gg c_D$, it can also be assumed that reaction (4) follows pseudo first-order kinetics with respect to the concentration of the analytes, and the rate equation for D_i is:

$$-\frac{d[D_i]}{dt} = k_i[D_i] \quad (i = 1, 2, \ldots, I) \quad (5)$$

Integration of Eq. (5) yields:

$$\Delta[D_i]_{t,D_i} = [D_i]_0 - [D_i]_t = [D_i]_0(1 - \exp(-k_i t)) \quad (6)$$

where $[D_i]_0$ is the initial concentration of D_i, $[D_i]_t$ is the concentration of D_i at time t, $\Delta[D_i]_{t,Di}$ is the concentration change at time, t, and k_i is the rate constant for D_i in reaction (5). Reactions (1) and (4) are competitive, and reaction (1) can be inhibited by D_i. Thus, A is oxidized and its concentration decreases much more as compared to that in the absence of D_i. Moreover, $\Delta[A]$ is proportional to the concentration of D_i [18]:

$$\Delta[A]_{t,1} - \Delta[A]_{t,2} = K\Delta[D_i]_{t,D_i} \quad (7)$$

where $\Delta[A]_{t,1}$ and $\Delta[A]_{t,2}$ are the concentration changes of A as the reaction progress without and with D_i, respectively, and K is the proportional coefficient of the inhibition effect of the D_i.

Combining the Eq. (7) with Eqs. (3) and (6), the following equation is obtained:

$$[A]_0(1 - \exp(-k_1 t))_1 - [A]_0(1 - \exp(-k_1 t))_2 = K[D_i]_0(1 - \exp(-k_i t)) \quad (8)$$

Assuming that only the absorbance of reagent A can be observed, according to Beer's law, the absorbance (Abs) of A at any wavelength and any time, t, is

$$\Delta Abs = K_i[D_i]_0 \quad (i = 1, 2, \ldots, I) \quad (9)$$

where K_i is the proportionality coefficient of D_i, and ΔAbs is the difference in absorbance A between the reactions without and with the analyte, D_i. Eq. (9) can be further simplified for I analytes:

$$\Delta Abs = \sum_{i=1}^{I} K_i c_{D_i} \quad (10)$$

For a set of M standard calibration samples ($\boldsymbol{C}_{M\times I}$), and their absorbance A values measured at a fixed wavelength at time, T, points ($t = 1, 2, \ldots, T$), the ΔAbs relationship (Eq. (10)) can be

expanded into a matrix form:

$$\Delta \boldsymbol{Abs} = \begin{bmatrix} A_{11} & A_{12} & \cdots & A_{1T} \\ A_{21} & A_{22} & \cdots & A_{1T} \\ \vdots & \vdots & & \vdots \\ A_{m1} & A_{m2} & \cdots & A_{MT} \end{bmatrix} = \begin{bmatrix} c_{11} & c_{12} & \cdots & c_{1I} \\ c_{21} & c_{22} & \cdots & c_{2I} \\ \vdots & \vdots & & \vdots \\ c_{m1} & c_{m2} & \cdots & c_{MI} \end{bmatrix} \times \begin{bmatrix} K_{11} & K_{12} & \cdots & K_{1T} \\ K_{21} & K_{22} & \cdots & K_{1T} \\ \vdots & \vdots & & \vdots \\ K_{I1} & K_{I2} & \cdots & K_{IT} \end{bmatrix} = \boldsymbol{C}_{M\times I}\boldsymbol{K}_{I\times T} \tag{11}$$

where $\boldsymbol{K}$ matrix is the proportional coefficient. Consequently, Eq. (11) allows one to resolve the kinetic system by suitable chemometrics methods without the knowledge of the detailed reaction mechanism.

2.2. Chemometrics methods

2.2.1. Multivariate calibration (PCR and PLS)

For multicomponent analysis, the calibration is carried out using known mixtures rather than individual analytes as in time-independent chemical systems, which has usually been used in kinetic methods [19,20]. As described above (Section 2.1), the application of multivariate calibration for multicomponent kinetic analyses involves the preparation of a set of mixtures of known compositions and the measurement of their absorbance at different time. Analytical relevant quantitative information of the system can be obtained with the use of one or the other of the two well known multivariate calibration methods, principal component regression (PCR) [21] and partial least squares regression (PLS) [22]; these methods use statistically significant orthogonal factors to build calibration models to estimate the linear relationship between the dependent ($\boldsymbol{C}_{M\times I}$) and independent ($\Delta\boldsymbol{Abs}_{M\times T}$) variables. The theory and principles of PCR and PLS are widely documented in the literature [23]. For this study, in PCR and PLS regression modeling, the first step involves the construction of calibrations for the quarternary mixture of hydroquinone, pyrocatechol, resorcin and phenol. The established models are then verified by predicting the composition of another set of unknown samples. Both PCR and PLS assume that there is a linear relationship between the absorbance measured and the concentrations of the components. The methods are flexible, and can account for some non-linearity and reduce interference problems or background noise.

In PCR [21], the absorbance data matrix $\boldsymbol{Abs} = \boldsymbol{CK}$ is broken down as:

$$\boldsymbol{Abs} = \boldsymbol{TP}^T + \boldsymbol{E} \tag{12}$$

where $\boldsymbol{Abs}$ is the absorbance intensity data matrix; the superscript 'T' denotes the transpose of the matrix, $\boldsymbol{T}$ and $\boldsymbol{P}^{\mathrm{T}}$ are the score and loading matrices which correspond with the absorbance matrix, and $\boldsymbol{E}$ is the residual matrix of $\boldsymbol{Abs}$. Here the $\boldsymbol{T}$ and $\boldsymbol{C}$ can be related with the coefficient matrix $\boldsymbol{G}$:

$$\boldsymbol{C} = \boldsymbol{TG} \tag{13}$$

Once the model has been fully developed, it can be used for the determination of the analyte concentrations by simply using the absorbance data set for the mixtures of the unknown concentration, and PCR to resolve the equation:

$$\boldsymbol{C}_{new} = \boldsymbol{Abs}_{new}\boldsymbol{PG} \tag{14}$$

where the $\boldsymbol{C}_{new}$ and $\boldsymbol{Abs}_{new}$ are the concentration and absorbance matrices of unknown mixtures, respectively.

For the PLS model [22], the concentration matrix is broken down into:

$$\boldsymbol{C} = \boldsymbol{UQ}^T + \boldsymbol{E} \tag{15}$$

where $\boldsymbol{U}$ and $\boldsymbol{Q}^T$ are the score and loading matrices of concentration matrix $\boldsymbol{C}$, and $\boldsymbol{E}$ is the residual matrix of $\boldsymbol{C}$.

$\boldsymbol{Abs}$ and $\boldsymbol{C}$ are mutually related by:

$$\boldsymbol{U} = \boldsymbol{TR} \tag{16}$$

where $\boldsymbol{R}$ is a diagonal regression matrix called the 'inner relationship'.

If the model is fully developed, it can be used for the determination of the analyte concentration by simply using the absorbance data set for unknown mixtures according to the equation:

$$\boldsymbol{C}_{new} = \boldsymbol{Abs}_{new}\boldsymbol{PRQ}^T \tag{17}$$

The major difference between the PCR and PLS is that, for the PCR method, only the information in the response matrix (here absorbance) is used in the data matrix decomposition; for the PLS method, the concentration data matrix is also used in the calibration model step.

2.2.2. Radial basis function artificial neural network (ANN)

Artificial neural network (ANN) is a powerful chemometric method because it does not need any model structure specification, and can process multivariate problems of nonlinear systems. ANN has been often applied for simultaneous determination of analytes in multicomponent problems [20,24]. With proper training, ANN can accurately model the presence of synergistic effects and avoid the potential loss of kinetic data for mixtures resulting from very short periods [25]. There are two main ANN methods – the radial basis function artificial neural network (RBF-ANN) and back propagation artificial neural network (BP-ANN); these have different transfer functions to solve complex systems. A kernel or basis function is classified as a local activation function compared to a sigmoid function. The main difference is that the latter defines an ellipsoid in the input space between the transfer function in the BP networks and the kernel function in the RBF networks. For successful implementation, it is important to find suitable centers for the RBF Gaussian function, which is characterized by two parameters – the center and peak width (c_j and σ_j). The output from the jth Gaussian neuron for an input object, $\boldsymbol{x}_i$ can be calculated by $o_j(x) = \exp(-||\boldsymbol{x}_j - c_j||^2/\sigma_j)$, where $||\boldsymbol{x}_j - c_j||$ is the calculated Euclidean distance between x_i.

In this work, the kinetic data obtained from the reaction were resolved by the RBF-ANN model, which has three types of layers: input, hidden and output [23]. The first layer has input nodes that transmit unweighted inputs to each node in the hidden layer; each hidden node contains a RBF as the transfer function, and the outputs of these nodes are weighted and summed to produce the final output.

The output nodes, which compute the weighted sum of the hidden node outputs, are

$$y_i = \sum_{i=1}^{n} w_{ji} o_j(x) \tag{18}$$

where w_{ji} represents the weights of the connection between the hidden layer, i, and output layer, j, and $o_j(x)$ is obtained from above.

3. Experimental

3.1. Apparatus

The spectrophotometric analysis of phenolic components was carried out on an Agilent 8453 UV–visible spectrophotometer with

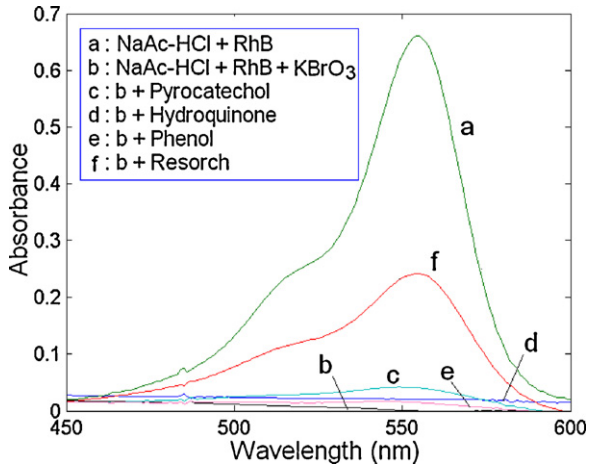

Fig. 1. UV–vis absorption spectra. (a) NaAc–HCl + RhB; (b) NaAc–HCl + RhB + $KBrO_3$; (c) NaAc–HCl + RhB + $KBrO_3$ + pyrocatechol (0.4 g mL^{-1}); (d) NaAc–HCl + RhB + $KBrO_3$ + hydroquinone (0.4 g mL^{-1}); (e) NaAc–HCl + RhB + $KBrO_3$ + phenol (0.4 g mL^{-1}); (f) NaAc–HCl + RhB + $KBrO_3$ + resorcin (0.4 g mL^{-1}). Optimal experimental conditions: T = 25 °C, c_{RhB} = 6.80′10^{-6} mol L^{-1}, c_{KBrO_3} = 2.34′10^{-6} mol L^{-1}, and pH = 3.0 (NaAc–HCl).

a 1.0 cm quartz cell. All measurements were performed with a thermostat cell compartment at 25 ± 0.5 °C with the aid of a Model ZC-10 (Ningbo Tianheng Instruments Factory, China) temperature control accessory. An Orion SA 720 digital pH-meter was used for pH adjustment; it was equipped with an Ag–AgCl glass combination pH electrode. All the solution volumes which were less than 1.0 mL were delivered with micropipettes (Finnpipette, Labsystems, Finland), and a stop watch was used to monitor the cell heating time.

The HPLC measurements were performed on an Agilent 1100 series HPLC-DAD system equipped with a vacuum degasser, quaternary pump, autosampler, injector with a 20 μL loop, an Agilent Zorbax eclipse XDB-C18 column (4.6 mm × 250 mm, 5 μm) with an Agilent Zorbax high pressure reliance cartridge guard-column (C18, 12.5 mm × 4.6 mm, 5 μm) and a DAD detector. The HPLC system was operated at 25 ± 0.5 °C.

The obtained chromatograms and kinetic curves were recorded and processed by a computer with programs written in MATLAB 6.5 (Mathworks).

3.2. Solution and reagents

The stock solutions (1.10 g L^{-1}) of pyrocatechol, resorcin, hydroquinone and phenol were prepared by dissolving 0.1100 g of each of these compounds with water in a 100 mL volumetric flask, and storing them in the dark at 4 °C. The UV spectra of these solutions (Fig. 1) show that for mixtures of these compounds, the spectra would seriously overlap, and the sensitivity for some compounds is quite low. The RhB stock solution (1.0×10^{-4} mol L^{-1}) was obtained by dissolving 0.0048 g RhB (M = 479.02 g mol^{-1}) in water and diluted to the mark. The potassium bromate stock solution of 0.01 mol L^{-1} was prepared by dissolving 0.1607 g of the compound in water and diluting to the mark in a 100 mL volumetric flask. The HCl–NaAc buffer solution (pH = 3.0) was prepared by adding a suitable amount of 0.3 mol L^{-1} HCl into 0.1 mol L^{-1} NaAc solution; the pH was monitored by an SA-720 (Orion) digital pH-meter.

All chemicals and reagents used were of Analytical Reagent grade, and double distilled water was used throughout the experiments.

3.3. General procedure

For all spectrophotometric analysis, the analytes and any other reagents were added directly into the 1.0 cm cell with the use of micropipettes. A suitable amount of pyrocatechol, resorcin, hydroquinone or phenol solution (or their mixtures) was transferred into the cell, then in sequence, 0.170 mL of 1.0×10^{-4} mol L^{-1}. RhB solution, 0.50 mL NaAc–HCl buffer and an amount of distilled water as required, were added to give a total volume of 1.915 mL. The sample was kept on the cell stand for 1.5 min at 25 ± 0.5 °C, and 0.585 mL of potassium bromate solution was added to the cell to a total volume of 2.50 mL. The sample was then stirred and the UV–vis spectra were recorded from 190 to 900 nm, every 1 nm (total 711 wavelengths), at 2 s intervals during 300 s (total 151 time points).

3.4. Determination of pyrocatechol, resorcin, hydroquinone and phenol in real water samples

Four real water samples, including tap water, lake-water, laboratory effluent, and industrial waste water, were collected and analysed in this work. All water samples were treated as follows [26]: a 500 mL sample was collected and acidified with phosphoric acid (1–2 drops), and a 1 mL 0.1 mol L^{-1} $FeSO_4$ solution was used to eliminate the free chlorine and other oxidants. The pH of the samples was adjusted to 4.0 with H_3PO_4, then 1 mL $CuSO_4$ solution (0.1 mol L^{-1}) was added to inhibit microbial oxidation. The collected water samples were stored at 4 °C.

The samples were then prepared by using a standard distillation method [26]. A water sample (150 mL) and distilled water (50 mL) were placed into a distillation flask (250 mL) and a few zeolite chips were added to prevent bumping. This sample was then distilled until 150 mL of the distillate was collected. The distillate was treated as described in the general procedure.

3.5. HPLC procedure

20 μL of each sample (solution from Section 3.4) were injected and the concentrations were calculated on the basis of the peak area ratios of the standard solutions. HPLC analysis was carried out at a flow rate of 1.0 mL min^{-1} using a mobile phase of methanol and water (55:45, v/v); the detector was set at 277 nm. The mobile phase was prepared daily, filtered through a 0.45 μm membrane and sonicated before use. The retention time employed were 2.8 min for pyrocatechol, 3.2 min for resorcin, 2.5 min for hydroquinone and 4.4 min for phenol.

4. Results and discussion

4.1. Spectral characteristics and reaction kinetics

The UV–vis absorption spectra of pyrocatechol, resorcin, hydroquinone and phenol were collected with the use of an Agilent 8453 UV–visible spectrophotometer. The basic dye, RhB, displayed a broad and relatively intense spectrum when dissolved in the somewhat acidic buffer medium (Fig. 1a). However, when potassium bromate oxidizing agent was added to the RhB/buffer sample, the absorbance of the RhB spectrum decreased markedly because of the reaction of the dye and the oxidant [27]. Furthermore, in the presence of trace amounts of each of the compounds – pyrocatechol, resorcin, hydroquinone or phenol, the reaction rates decreased depending on the added substances (spectral curves b–e, Fig. 1). Also, the spectrophotometric kinetic data of the separate reactions for pyrocatechol, resorcin, hydroquinone and phenol were obtained at 557 nm overtime the time range of 0–300 s (see Fig. 2). Qualitative analysis of the absorbance vs time curves suggested that the highest reaction rate was with phenol and the slowest with

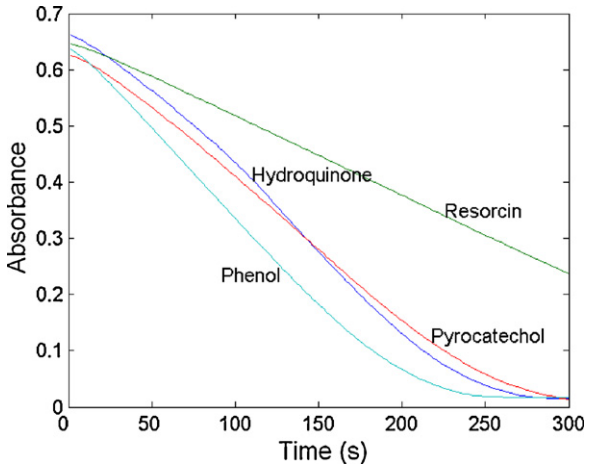

Fig. 2. Kinetic curves of pyrocatechol, resorcin, hydroquinone and phenol vs. time at 557 nm. Experimental conditions were as in Fig. 1.

resorcin, while hydroquinone and pyrocatechol were between the rate curves associated with the two former reagents. Arguably, the resorcin rate curve exhibited longer linear reaction rate behaviour (~50–300 s), while Phenol showed linear tendency approximately between 25 and 175 s.

4.2. Chemical reaction mechanism

The above spectral observations (Figs. 1 and 2) suggest that pyrocatechol, resorcin, hydroquinone and phenol have significant inhibitory effects on the redox reaction between RhB and potassium bromate. A possible suggested reaction mechanism is [28]:

$$BrO_3^- + RhB_{(Red)} + H^+ \rightarrow Br^- + RhB_{(Ox)} + H_2O \quad (19)$$

$$BrO_3^- + \text{phenolic component}_{(Red)} + H^+ \rightarrow Br^- + \text{phenolic component}_{(Ox)} + H_2O \quad (20)$$

where the $RhB_{(Ox)}$ and phenolic $component_{(Ox)}$ are the products of RhB and original phenolic component, respectively. The structures of the phenols were changed to benzoquinone when they were oxidized by potassium bromate [29,30].

4.3. The reaction conditions

For taking full advantage of the experimental procedure, various experimental conditions, such as the concentration of potassium bromate and RhB, the pH of the buffer and the reaction temperature, have been investigated.

The effect of pH on the analytical signal was studied in range of 1.5–5.0. The results showed that the response signal increases with increasing pH up to 3.0 and decreases at higher pH (>3.0). Therefore, pH 3.0 was selected for further study.

The influence of RhB or the $KBrO_3$ concentrations on the kinetic behaviour was investigated in the ranges of 0.4–1.6 × 10^{-6} mol L^{-1} for RhB, and 1.2–3.6 × 10^{-3} mol L^{-1} for $KBrO_3$. In the reaction, the amount of $KBrO_3$ was in excess, and the kinetics were assumed to follow the pseudo-first-order reaction model. It was found that the absorbance increased quickly with the increasing concentrations of RhB and potassium bromate, and maximum absorbance was found at 6.8 × 10^{-6} mol L^{-1} RhB and 2.34 × 10^{-3} mol L^{-1} $KBrO_3$; However, at higher concentrations, the signal intensity decreased with increasing concentrations.

The effect of temperature on the analytical signal was studied in the range of 20–60 °C with the optimum of reagent concentrations described above. The signal increased with temperature up to 25 °C, and almost no change was observed at higher temperatures. Thus, 25 °C was selected as the optimum.

4.4. Calibration of individual analyte

Under the above optimum conditions, the kinetic curves (Fig. 3) were recorded at the analytical wavelength, 557 nm, for pyrocatechol, resorcin, hydroquinone and phenol at different concentrations, respectively. The figures of merit for calibrations of each analyte are summarized in Fig. 3 (see insert plots). Kinetic data were collected between 0 and 300 s reaction time, and the correlation coefficients suggested good linearity within the concentration range of 0.22–3.30 μg mL^{-1} for pyrocatechol, 0.108–0.828 μg mL^{-1} for resorcin, 0.36–3.96 μg mL^{-1} for hydroquinone, and 1.52–19.76 μg mL^{-1} for phenol.

4.5. Calibration and prediction sets

In order to extract maximum quantitative information about the samples with the use of minimum experimental trials, the orthogonal array design was applied for the construction of the calibration set. A set of samples was prepared according to a four-level orthogonal array design, denoted by $OA_{16}(4^4)$ [31]. The ranges of concentration were 0.264–1.584 μg mL^{-1} for pyrocatechol, 0.115–0.547 μg mL^{-1} for resorcin, 0.432–2.592 μg mL^{-1} for hydroquinone, and 1.824–10.944 μg mL^{-1} for phenol (see Table 2). The absorbance of these samples was measured by the kinetic spectrophotometric method described above, and the kinetic absorbance response matrix, ***Abs*** (16 × 301), and concentration matrix, ***C*** (16 × 4), were then recorded and processed by suitable multivariate calibration (PCR and PLS) and artificial neural net works (RBF-ANN) methods to establish the calibration models.

Another set of sixteen quarternary mixtures was prepared with different analyte concentrations from the samples employed in the calibration set in order to verify the calibration models. A full factorial design was applied, and the selected concentrations for this set were similar to those of the calibration set. The composition of the prediction samples is also shown in Table 2. Estimates of uncertainty of each analyte from the prediction set were made with the use of the relative prediction errors (RPE) according to Eqs. (15) and (16) below [32].

The RPE_S, for a single component in mixtures is

$$RPE_S = \left[\frac{\sum_{i=1}^{n} (c_{ij(\text{found})} - c_{ij(\text{added})})^2}{\sum_{i=1}^{n} (c_{ij(\text{added})})^2} \right]^{0.5} \quad (21)$$

and the RPE_T for all components can be formulated as:

$$RPE_T = \left[\frac{\sum_{i=1}^{n}\sum_{j=1}^{m} (c_{ij(\text{found})} - c_{ij(\text{added})})^2}{\sum_{i=1}^{n}\sum_{j=1}^{m} (c_{ij(\text{added})})^2} \right]^{0.5} \quad (22)$$

where $c_{ij(\text{added})}$ indicates the concentration of jth component in jth mixtures and $c_{ij(\text{found})}$ is its estimate found from the analysis.

The prediction results for the verification data found with the aid of the different chemometric methods are summarized in Table 3. The RPE_T values from the application of the PCR, PLS and RBF-ANN calibrations are very similar, but the RBF-ANN model performs slightly better than the PLS one with the PCR performing relatively poorly. Most likely, RBF-ANN performed better because it can accommodate well any non-linear contributions in the calibration data modeling [33]. Thus, the RBF-ANN calibration model was chosen for the simultaneous determination of the four phenols in the various water samples.

4.6. Interference study

To investigate the selectivity of the proposed method, the effect of various substances on the determination of the analytes,

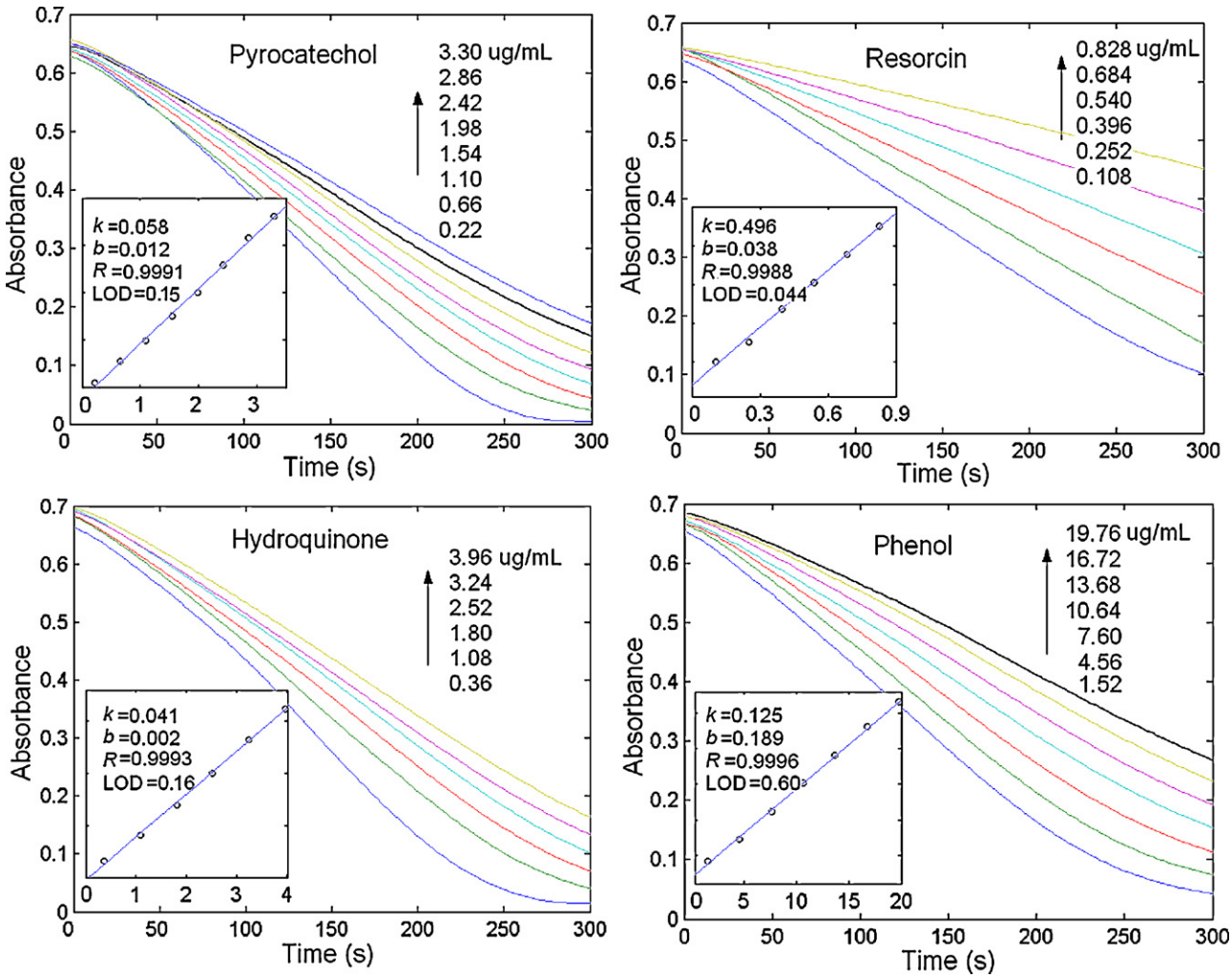

Fig. 3. Kinetic curves of pyrocatechol, resorcin, hydroquinone and phenol with different concentrations ((g mL^{-1}); spectral data were collected at λ_{max} = 557 nm. Experimental conditions were as in Fig. 1.

a mixture containing 0.20 μg mL^{-1} of resorcin and phenol, and 0.40 μg mL^{-1} of pyrocatechol and hydroquinone was tested under the optimum conditions, and the concentration of the phenolic analytes were predicted by the RBF-ANN model. Several representative potential interferents such as inorganic cations, anions and molecular compounds were investigated individually for their effect on the phenols' mixture and the subsequent spectra. The concentration of the tested interferent was increased until an RPE_T of 10% was reached for the determination of a mixture of the four phenols. The maximum concentration of interfering species that could be tolerated was selected as that which produced an RPE_T of just below 10% as defined above, and the tolerance levels were expressed

Table 2
Composition of calibration and predication sets of pyrocatechol, resorcin, hydroquinone and phenol (μg mL^{-1}).

No.	Calibration set (μg mL^{-1})				Predication set (μg mL^{-1})			
	Pyrocatechol	Resorcin	Hydroquinone	Phenol	Pyrocatechol	Resorcin	Hydroquinone	Phenol
1	0.264	0.115	0.423	1.824	0.352	0.122	0.576	2.432
2	1.584	0.547	1.872	1.824	1.474	0.511	1.800	2.432
3	0.704	0.115	1.152	4.864	0.726	0.122	1.188	5.016
4	1.144	0.547	2.597	4.864	1.100	0.511	2.412	5.016
5	1.144	0.115	1.872	7.904	1.100	0.122	1.800	7.600
6	0.704	0.547	0.432	7.904	0.726	0.511	0.576	7.600
7	1.584	0.115	2.597	10.944	1.474	0.122	2.412	10.184
8	0.264	0.547	1.152	10.944	0.352	0.511	1.188	10.184
9	0.264	0.259	1.872	4.864	0.352	0.252	1.800	5.016
10	1.584	0.403	0.432	4.864	1.474	0.382	0.576	5.016
11	0.704	0.259	2.592	1.824	0.726	0.252	2.412	2.432
12	1.144	0.403	1.152	1.824	1.100	0.382	1.188	2.432
13	1.144	0.259	0.432	10.944	1.100	0.252	0.576	10.184
14	0.704	0.403	1.872	10.944	0.726	0.382	1.800	10.184
15	1.584	0.259	1.152	7.904	1.474	0.252	1.188	7.600
16	0.264	0.403	2.592	7.904	0.352	0.382	2.412	7.600

Table 3
Prediction results of synthetic samples by different chemometric methods.

Chemometrics	%RPE$_s$				%RPE$_T$
	Pyrocatechol	Resorcin	Hydroquinone	Phenol	
PLS (4)[a]	10.45 (105)[b]	8.41 (104)	11.36 (114)	6.35 (104)	6.8
PCR (4)[a]	8.95 (106)	8.48 (103)	11.44 (114)	7.11 (105)	7.4
RBF-ANN (6, 480)[c]	8.50 (106)	9.48 (105)	8.29 (111)	6.5 (103)	6.7

[a] Values in the parentheses correspond to the number of factors used for PCR and PLS models.
[b] Values in the parentheses are mean Recoveries (%).
[c] Values in parentheses correspond to nodes in the hidden layer and the spread coefficient (SC), respectively.

Table 4
Results of phenolic compounds in water samples by the proposed method ($\mu g\,mL^{-1}$).

Samples[a]	Found		Added	Found after addition		Recovery (%)	
	ANN	HPLC		ANN	HPLC	ANN	HPLC
1. Lake water[c]							
Pyrocatechol	–[b]	–	0.60	0.65 ± 0.02[c]	0.57 ± 0.01	108	95
Resorcin	–	–	0.60	0.58 ± 0.01	0.58 ± 0.01	97	97
Hydroquinone	–	–	0.55	0.51 ± 0.01	0.60 ± 0.03	93	109
Phenol	–	–	7.00	6.99 ± 0.04	7.20 ± 0.18	100	103
2. Tap water[c]							
Pyrocatechol	–	–	0.60	0.59 ± 0.01	0.59 ± 0.01	98	98
Resorcin	–	–	0.80	0.77 ± 0.01	0.76 ± 0.01	96	95
Hydroquinone	–	–	0.50	0.40 ± 0.01	0.56 ± 0.02	80	112
Phenol	–	–	4.00	3.60 ± 0.03	3.70 ± 0.06	90	93
3. Industrial waste water							
Pyrocatechol	0.45 ± 0.02	0.41 ± 0.01	0.30	0.71 ± 0.01	0.74 ± 0.02	95	104
Resorcin	0.51 ± 0.02	0.52 ± 0.01	0.20	0.75 ± 0.02	0.70 ± 0.02	105	97
Hydroquinone	0.24 ± 0.01	0.29 ± 0.01	0.20	0.40 ± 0.01	0.52 ± 0.01	91	106
Phenol	4.76 ± 0.04	4.80 ± 0.02	3.00	8.47 ± 0.04	8.21 ± 0.07	109	105
4. Laboratory effluents							
Pyrocatechol	0.49 ± 0.01	0.44 ± 0.01	0.20	0.64 ± 0.01	0.62 ± 0.02	93	97
Resorcin	0.64 ± 0.02	0.65 ± 0.02	0.10	0.83 ± 0.01	0.78 ± 0.02	112	104
Hydroquinone	0.36 ± 0.03	0.41 ± 0.01	0.20	0.51 ± 0.02	0.54 ± 0.01	91	89
Phenol	2.64 ± 0.05	2.50 ± 0.02	2.00	4.49 ± 0.08	4.37 ± 0.07	97	97

[a] Lake water was taken from the 'Dragon Lake' on the Nanchang University campus; Industrial waste water was collected from a paper mill in Nanchang city.
[b] Not detected.
[c] Mean value of three determinations ±standard deviations.

as tolerance ratios (TL), i.e. mg of interferent per mL of phenols ($w_{Interf}/w_{Resorcin}$ was used here, and resorcin was selected as a reference). The TL results were: 750 – NH_4^+, Zn^{2+}, Fe^{3+}, Cl^-, SO_4^{2-}, NO_3^-; 400 – K^+, Na^+, Co^{2+}, Br^-, As^{3+}, methanol, ethanol; 50 – Mg^{2+}, Ca^{2+}, Pb^{2+}, Cr^{3+}, Al^{3+}, tartrate, sorbate; 20 – Mn^{2+}, Hg^{2+}, I^-; 5 – ascorbic acid, glucose.

The TL values suggest that common ions such as K^+, Na^+, NH_4^+, SO_4^{2-}, Cl^- were least intrusive (TL ~ 750–400), while ascorbic acid and glucose (TL ~ 5), were the most strong interferents. There are other compounds, which may be present in the samples and could be expected to interfere with the analysis; they include bisphenol A, chlorophenol and nonylphenol, but these are insoluble in water, and xylenol is practically insoluble in acid and will be decomposed when heated. Thus, for real water samples, most of these potentially interfering substances could be removed during the distillation step in the procedure (Section 3.4) and their interferences eliminated.

4.7. Analysis of water samples

In order to evaluate the applicability of the proposed method, the four phenols were analysed simultaneously in various water samples with the aid of the RBF-ANN calibration model. Since the level of these compounds is generally low in water samples, the analyte samples were spiked appropriately. The results (Table 4) indicated that relatively high amounts of these compounds were found in the industrial effluents and laboratory waste water but not in the lakes and tap water. Also, the performance of the method was compared with the results from the reference HPLC procedure with the use of the %Recovery criterion. The results were very similar with both methods performing satisfactorily.

5. Conclusion

In this work, a novel and sensitive kinetic – spectrophotometric method, based on the inhibition of the oxidative reaction of RhB by potassium bromate by phenols, was successfully applied for the simultaneous determination of pyrocatechol, resorcin, hydroquinone and phenol in mixtures. Multivariate calibrations with the use of PCR, PLS and RBF-ANN methods were compared, and the prediction performance based on the %RPE$_T$ criterion (7.4–6.7%), was found to be quite similar between models although the RBF-ANN one was slightly better than the other two. This model was then used to analyse the four phenol analytes in four different types of water sample, and the analytical performance was found to be satisfactory when compared with the results from the reference HPLC procedure. Thus, the proposed method is a convenient and inexpensive alternative analytical method for the simultaneous determination of phenolic compounds in various types of waters.

Acknowledgements

The authors gratefully acknowledge the financial support by the National Natural Science Foundation of China (No. NSFC-

21065007), and the State Key Laboratory of Food Science and Technology of Nanchang University (SKLF-MB-201002 and SKLF-TS-200919).

References

[1] P. Patnaik, A Comprehensive Guide to the Hazardous Properties of Chemical Substances, 3rd ed., John Wiley & Sons, 2007, p. 821.
[2] J. Adamski, P. Nowak, J. Kochana, Simple sensor for the determination of phenol and its derivatives in water based on enzyme tyrosinase, Electrochim. Acta 55 (2010) 2363–2367.
[3] A. Svobodova, J. Psotova, D. Walterova, Natural phenolics in the prevention of UV-induced skin damage. A review, Biomed. Papers 147 (2003) 137–145.
[4] A.J.S. Ahammad, S. Skarker, M.A. Rahman, J.J. Lee, Simultaneous determination of hydroquinone and catechol at an activated glassy carbon electrode, Electroanalysis 22 (2010) 694–700.
[5] J. Fan, T. Zhang, J.H. Sun, M.H. Fan, Kinetic fluorimetric measurement of trace resorcin in phenol mixtures, J. Fluoresc. 17 (2007) 113–118.
[6] N.A. Penner, P.N. Nesterenko, A.M. Rybalko, Use of Hypercrosslinked polystyrene for the determination of pyrocatechol, resorcin, and hydroquinone by the reversed-phase HPLC with dynamic on-line preconcentration, J. Anal. Chem. 56 (2001) 934–939.
[7] A.R. Sousa, M.A. Trancoso, Validation of an environmental friendly segmented flow method for the determination of the phenol index in waters as alternative to the conventional one, Talanta 79 (2009) 796–803.
[8] F.M. Lancas, I.R. Olivares, P.M. Alves, Development, validation and application of a method to analyze phenols in water samples by solid phase micro extraction-gas chromatography-flame ionization detector, J. Environ. Sci. Health B 42 (2007) 491–498.
[9] S. Waidyanatha, N. Rothman, G. Li, M.T. Smith, S. Yin, S.M. Rappaport, Rapid determination of six urinary benzene metabolites in occupationally exposed and unexposed subjects, Anal. Biochem. 327 (2004) 184–199.
[10] J. Witting, S. Wittemer, M. Veit, Validated method for the determination of hydroquinone in human urine by high-performance liquid chromatography-coulometric-array detection, J. Chromatogr. B 761 (2001) 125–132.
[11] P.L. Garcia, M.I.R.M. Santoro, E.R.M. Kedor-Hackman, A.K. Singh, Development and validation of a HPLC and a UV derivative spectrophotometric methods for determination of hydroquinone on gel and cream preparations, J. Pharm. Biomed. Anal. 39 (2005) 764–768.
[12] C. Desiderio, L. Ossicini, S. Fanali, Analysis of hydroquinone and some of its ethers by using capillary electrochromatography, J. Chromatogr. A 887 (2000) 489–496.
[13] R.M. de Carcalho, C. Mello, L.T. Kubota, Simultaneous determination od phenol isomers in binary mixtures by differential pulse voltammetry using carbon fibre electrode and neural network with pruning as a multivariate calibration tool, Anal. Chim. Acta 420 (2000) 109–121.
[14] M.I. Sirajuddin, A. Bhanger, A. Niaz, A. Shah, Rauf, Ultra-trace level determination of hydroquinone in waste photographic solutions by UV–vis spectrophotometry, Talanta 72 (2007) 546–553.
[15] K.O. Lupetti, F.R.P. Rocha, O. Fatibello-Filho, An improved flow system for phenols determination exploiting multicommutation and long pathlength spectrophotometry, Talanta 62 (2004) 463–467.
[16] B.M. Quencer, S.R. Crouch, Multicomponent kinetic methods, Crit. Rev. Anal. Chem. 24 (1993) 243–262.
[17] P. Lu, L.M. Kong, J. Wu, Simultaneous analysis of phenolic mixtures in water by high performance liquid chromatography, J. Yangzhou Univ. (Natural Science Edition) 4 (2004) 24–26.
[18] X.J. Cui, G.Z. Fang, L.Q. Jiang, S. Wang, Kinetic spectrophotometric method for rapid determination of trace formaldehyde in foods, Anal. Chim. Acta 590 (2007) 253–259.
[19] M.A. Karimi, M.H. Mashhadizadeh, M. Mazloum Ardakani, N. Sahraei, Simultaneous kinetic-potentiometric determination of levodopa and carbidopa using multivariate calibration methods, J. Food Drug Anal. 5 (2008) 39–47.
[20] M. Chamsaz, A. Safavi, J. Fadaee, Simultaneous kinetic-spectrophotometric determination carbidopa, levoldopa, and methyldopa in presence of citrate with the aid of multivariate calibration and artificial neural networks, Anal. Chim. Acta 603 (2007) 140–146.
[21] D.M. Haaland, E.V. Thomas, Comparison of multivariate calibration methods for quantitative spectral analysis, Anal. Chem. 62 (1990) 1091–1099.
[22] P. Geladi, B.R. Kowalski, Partial least-squares regression: a tutorial, Anal. Chim. Acta 185 (1986) 1–17.
[23] Y.N. Ni, The Application of Chemometrics in Analytical Chemistry, Chinese Science Press, Beijing, 2004.
[24] N. Chu, S.H. Fan, Sequential injection kinetic spectrophotometric determination of quarternary mixtures of carbamate pesticides in water and fruit samples using artificial neural networks for multivariate calibration, Spectrochim. Acta A 74 (2009) 1173–1181.
[25] M. Hasani, L. Yaghoubi, H. Abdollahi, A kinetic spectrophotometric method for simultaneous determination of glycine and lysine by artificial neiral networks, Anal. Biochem. 365 (2007) 74–81.
[26] HJ 503-2009, Water quality-Determination of volatile phenolic compounds-4-AAp spectrophotometric method, Branch of Environmental Protection, People's Republic of China, 2009.
[27] X.S. Zhu, Y.Q. Zhang, Inhibition kinetic determination of trace amount of iodide by the spectrophotometric method with rhodamine B, Spectrochim. Acta A 70 (2008) 510–513.
[28] J. Fan, X.J. Shao, H.X. Xu, S.L. Feng, A novel inhibitory kinetic fluorimetric method for the determination of trace methomyl in environmental samples, Luminescence 24 (2009) 266–270.
[29] P. Kumar, H. Nikakhtari, M. Nemati, G. Hill, J. Headley, Oxidation of phenol in a bioremediation medium using chlorine dioxide, J. Chem. Technol. Biotechnol. 85 (2010) 720–725.
[30] M.D.T. Sotomayor, A.A. Tanaka, L.T. Kubota, Development of an enzymeless biosensor for the determination of phenolic compounds, Anal. Chim. Acta 455 (2002) 215–223.
[31] W.G. Lan, M.K. Wong, N. Chen, Y.M. Sin, Orthogonal array design as a chemometric method for the optimization of analytical procedures. Part 2. Four-level design and its application in microwave dissolution of biological samples, Analyst 119 (1994) 1669–1675.
[32] M. Otto, W. Wegscheider, Spectrophotometric multicomponent analysis applied to trace metal determinations, Anal. Chem. 57 (1985) 63–69.
[33] M. Bahram, A. Afkhami, Recent applications of kinetic methods in multicomponent analysis, J. Iran. Chem. Soc. 5 (2008) 352–366.